Adsorption of linear polymers on impenetrable fractal boundaries of checkerboard fractal lattices

Sava Milošević,[1] Ivan Živić,[2] and Vladimir Miljković[1]
[1]*Faculty of Physics, University of Belgrade, P.O. Box 368, 11001 Belgrade, Serbia*
[2]*Faculty of Natural Sciences and Mathematics, University of Kragujevac, 34000 Kragujevac, Serbia*
(Received 19 June 1996)

We study the problem of adsorption of linear chain polymers situated in fractal containers that belong to the checkerboard fractal family, as well as the case of the closely related family of X fractals. Each member of any of the two families has a fractal impenetrable adsorbing boundary, and can be labeled by an odd integer b ($3 \leqslant b \leqslant \infty$). By applying the exact and Monte Carlo renormalization group method, we calculate the critical exponent ϕ, associated with the number of adsorbed monomers, for a sequence of fractals with $3 \leqslant b \leqslant 81$. We find that, in the region studied, ϕ monotonically decreases with the increase of b (that is, with increase of the container fractal dimension d_f). In addition, we observe that the obtained results are qualitatively the same as in the case of fractals with Euclidean adsorbing boundaries, while the established quantitative differences can be ascribed to the fact that the fractal nature of boundaries do enhance the polymer adsorption process. Finally, we establish that the adsorption enhancement does not depend on specific variations of the sets of monomer-wall interactions. [S1063-651X(97)04604-7]

PACS number(s): 36.20.Ey, 64.60.Ak, 05.50.+q

I. INTRODUCTION

Physics of a polymer chain in a good solvent near an impenetrable wall (boundary) with short-range attractive forces has been extensively studied because of its practical importance [1], and as a challenging problem within the modern theory of critical phenomena [2]. The most frequently applied model for a polymer chain has been the self-avoiding random walk model (SAW), so that steps of the walk have been identified with monomers that comprise the polymer, while the homogeneous solvent surrounding has been represented by a Euclidean lattice. Under these assumptions, the problem of polymer adsorption has been attacked by various theoretical methods, such as the mean-field approach, Monte Carlo simulations, and the conformal invariance method, including certain simplifications (as the concept of a directed polymer). Despite many studies, the polymer adsorption phenomenon, in the case of Euclidean lattices with homogeneous impenetrable boundaries, has been an active research problem. For example, the crossover critical exponent ϕ, associated with the number M of adsorbed monomers, has been predicted, by the conformal invariance method [3], to have the value 1/2 for two-dimensional Euclidean lattices. This value has been a topic of numerous investigations [4–9], which have culminated in rigorous proof achieved via an exact study of the $O(n)$ loop model on the honeycomb lattice [10].

Unfamiliar difficulties as regards the polymer adsorption problem may appear in the case when the polymer-solvent system is enclosed within a fractal container, which, to make things more difficult, may have an impenetrable fractal boundary. Such a situation can be approached by the SAW model located on a deterministic fractal lattice bounded by an adsorbing wall. The corresponding problem has been first attacked by Bouchaud and Vannimenus [11] who established phenomenological bounds for the crossover exponent ϕ. To test the proposed bounds, Bouchaud and Vannimenus [11] have initiated the renormalization group (RG) approach to the problem and calculated ϕ for the two-dimensional and three-dimensional Sierpinski gasket (SG) lattices (with base $b=2$, in both cases). The knowledge of the critical exponent ϕ is of fundamental importance because it is a requisite for the assessment of the majority of observable physical quantities that appear in the adsorption problem. For this reason, the introduced RG approach [11] has been extended to other fractal cases [12–16]. The obtained results revealed intriguing facts concerning the dependence of ϕ on the characteristics of underlying fractal lattices and their adsorbing boundaries, which call forth new studies under similar lines.

In this paper, we study the polymer adsorption problem in the case of the infinite family of the checkerboard (CB) fractals, as well as the case of the closely related family of X fractals. The peculiarity of the CB and X fractal families is the fact that each member of any of the two families has a fractal impenetrable boundary. We have applied the exact renormalization group and Monte Carlo renormalization group (MCRG) method to calculate the crossover exponent ϕ for large sequences of both fractal families. The obtained results provide a new large set of data needed for possible identification of a finite number of fractal properties, which determine characteristics of the polymer adsorption phenomenon, and, in particular, those properties which determine the value of the critical exponent ϕ. More specifically, the obtained results allow us to test the validity of the phenomenologically established bounds [11], and a closed-form expression [13], for ϕ formulated in terms of the container fractal dimension d_f, the adsorption wall fractal dimension d_s, and the end-to-end distance critical exponent ν_B (for the polymer in the desorbed-bulk state). Besides, the cases under study allow us to discuss the influence of particular shapes of the impenetrable adsorbing boundaries and the pertaining sets of monomer-wall interactions on possible values of the crossover exponent ϕ.

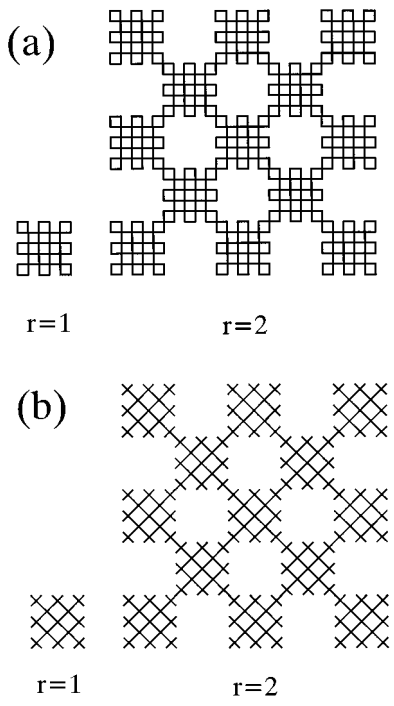

FIG. 1. The first two steps ($r=1$ and $r=2$) of the self-similar construction of the CB (a) and X (b) fractals, in the case $b=5$.

This paper is organized as follows. In Sec. II we first describe the CB and X fractals and present the general framework of the RG method for studying the polymer adsorption problem on these fractals, in a way that should make the method transparent for exact calculations, as well as for the Monte Carlo calculations. In Sec. III we give details of the relevant calculations and results for the critical exponent ϕ for a sequence of the fractals under study. Discussion of the obtained results and their relevance to the current knowledge of the polymer adsorption phenomena are given in Sec. IV.

II. FRAMEWORK OF THE RENORMALIZATION GROUP APPROACH

The RG calculation of the crossover exponent for the adsorption problem on the CB fractals is, in principle, similar to the previous applications of the RG method to the studies of the same problem on other families of deterministic fractals [12–16]. However, the implementation of the RG method for the CB fractals is more complex and requires additional elucidation. Before going into pertinent details, we shall briefly describe the structure of the CB and the related X fractals.

Each member of the plane CB and X family is labeled by an odd integer $b \geq 3$ and can be obtained as the result of an infinite iterative process of successive ($r \rightarrow r+1$) enlarging the fractal structure b times and replacing the smallest parts of the enlarged structure with the generator (initial structure, $r=1$). The generator of a CB fractal is a square, of size $b \times b$, composed of b rows of unit squares, so that within each row and each column every other of them is removed, whereas in the case of X fractals instead of unit squares we put crosses composed of squares' diagonals (see Fig. 1).

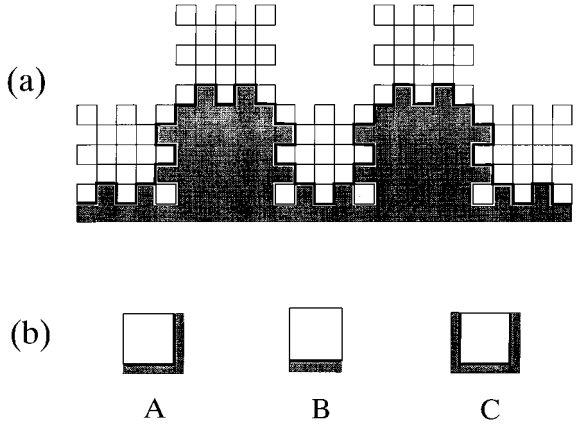

FIG. 2. (a) The impenetrable wall (the shaded region) with the adsorbing fractal boundary (heavy line) of the $b=5$ member of the CB fractal family, at the second stage of construction. One should observe that, in this case, there are four elementary squares whose edges are not included in the boundary because such squares would represent dead ends for adsorbed polymer modeled by a never-starting and never-ending SAW. (b) The three types of elements that comprise the fractal boundaries of the CB fractals.

Taking into account the self-similar way of the construction of the fractals, one can easily show that the fractal dimension d_f for an arbitrary CB fractal (as well as for X), specified by b, is equal to $\ln[(b^2+1)/2]/\ln b$, so that d_f acquires the Euclidean value 2 when $b \rightarrow \infty$.

To study the polymer adsorption problem on the CB and X fractals, it is necessary to determine precise characteristics of their impenetrable fractal boundaries. It is convenient to assume that the adsorbing boundaries are the lower sides of the corresponding fractals, and, as an example, in Fig. 2 we depict the boundary of the $b=5$ CB fractal at the second ($r=2$) stage of construction. From this figure, it follows that the adsorbing boundaries can be conceived as fractal chains comprised of three types of elements A, B, and C. Mass m of such a chain, on a scale of length ℓ, is given by

$$m \sim \ell^{d_s}, \tag{2.1}$$

where d_s is the corresponding fractal dimension. If, on the rth stage of the fractal construction, we assume that the elements A, B, and C have the masses $m_A^{(r)}$, $m_B^{(r)}$, and $m_C^{(r)}$, respectively, we can write (in the case $b=5$) the recursion relations

$$m_A^{(r+1)} = 3m_A^{(r)} + 2m_B^{(r)} + 2m_C^{(r)}, \tag{2.2a}$$

$$m_B^{(r+1)} = 2m_A^{(r)} + 2m_B^{(r)} + m_C^{(r)}, \tag{2.2b}$$

$$m_C^{(r+1)} = 4m_A^{(r)} + 2m_B^{(r)} + 3m_C^{(r)}. \tag{2.2c}$$

Owing to the self-similarity of the fractal boundary chain, one may assume the following behavior for large r:

$$\frac{m_A^{(r+1)}}{m_A^{(r)}} \sim \frac{m_B^{(r+1)}}{m_B^{(r)}} \sim \frac{m_C^{(r+1)}}{m_C^{(r)}} \sim \lambda. \tag{2.3}$$

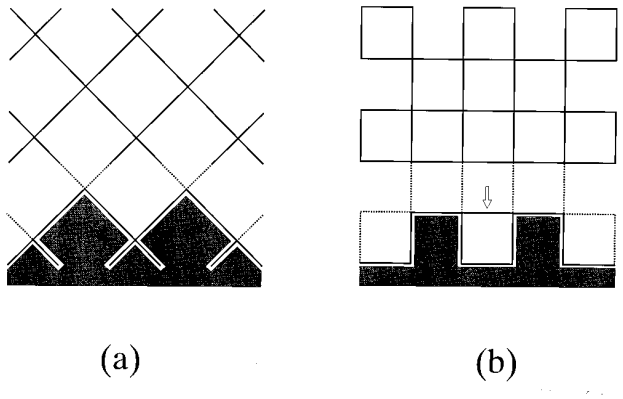

FIG. 3. The adsorbing walls (shaded regions) in the case of the X (a) and CB (b) fractals, for $b=5$. The SAW steps (monomers) along the bonds that comprise the adsorbing boundaries are weighted by xw. On the other hand, the SAW steps along the bonds (dotted lines) which lie in the layer adjacent to the boundary are weighted by the factor xt. Besides, in the case of the CB fractals there are bonds (marked by the downward oriented arrow in the figure) which appear as bridges over unit holes, and if a SAW step performed over such a bond it is weighted by xu. Finally, any SAW step above the adsorbing boundary and its contiguous layer is weighted by x.

The system of recursion relations (2.2) can have nonzero solutions of the type (2.3) only in the case $\lambda=7$, which, in conjunction with Eq. (2.1), yields $d_s=\ln 7/\ln 5$. This analysis can be performed quite similarly for $b>5$ (in both cases, that is, for CB and X fractals), so that for arbitrary b one can infer the general formula

$$d_s=\frac{\ln(2b-3)}{\ln b}. \tag{2.4}$$

We describe equilibrium properties of a linear polymer in a good solvent by the self-avoiding walk model, which is a random walk that must not contain self-intersections. In the terminology that applies to the SAW, we assign the weight x (fugacity) to each step in the bulk (away from the adsorbing boundary) and the weight xw to each step performed on the boundary. Here w is the Boltzmann factor $w=e^{-\epsilon_w/kT}$, where ϵ_w is the energy of a monomer lying on the adsorbing wall, and kT is the product of the Boltzmann constant and the temperature of the solvent. The fractal structure of the adsorbing boundary of the X and CB fractals (see Fig. 3) makes it necessary to introduce two additional weighting factors $t=e^{-\epsilon_t/kT}$ and $u=e^{-\epsilon_u/kT}$, with the respective monomer-wall interactions ϵ_t and ϵ_u. Accordingly, xt is the weight of those steps that are performed in the layer adjacent to the wall, while xu is the weight of the steps along the bonds that appear as bridges over unit holes on the adsorbing wall. The number of the adsorbed monomers (steps) M is a function of temperature T and its relation to the total number of monomers N is assumed to be

$$M\sim\begin{cases} N(T_a-T)^{1/\phi-1}, & T<T_a \\ N^{\phi}, & T=T_a \\ (T-T_a)^{-1}, & T>T_a \end{cases} \tag{2.5}$$

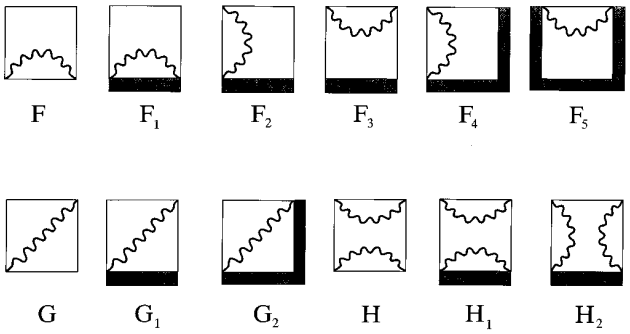

FIG. 4. Schematic representation of the twelve restricted partition functions used in describing all possible polymer configurations within the rth stage CB and X fractal structure. Thus, for example, F_1 represents a part of the polymer chain (wiggled solid line) which starts at the lower left vertex that lies on the adsorption wall, and exits at the lower right vertex that also lies on the adsorption wall. The interior details of the rth order fractal structure is not shown (it is manifested by the writhing of the solid line).

where T_a is the critical temperature of the adsorption, and ϕ is the crossover exponent [2,17]. It follows that, for temperatures higher than T_a, one should expect a vanishingly small fraction of monomers adsorbed at the surface, whereas for $T<T_a$ there should appear a finite fraction of adsorbed monomers.

In order to describe all possible configurations of chain polymers on the CB (X) fractals, it is necessary to introduce 12 restricted partition functions, which we divide into three sets $\{F\}$, $\{G\}$, and $\{H\}$ (see Fig. 4). The desorbed state of a polymer can be described by the three functions $F^{(r)}$, $G^{(r)}$, and $H^{(r)}$, whose recursion relations, for arbitrary b, should be of the polynomial form

$$F^{(r+1)}=\sum_{i,j,k} f(i,j,k)F^{(r)i}G^{(r)j}H^{(r)k}, \tag{2.6a}$$

$$G^{(r+1)}=\sum_{i,j,k} g(i,j,k)F^{(r)i}G^{(r)j}H^{(r)k}, \tag{2.6b}$$

$$H^{(r+1)}=\sum_{i,j,k} h(i,j,k)F^{(r)i}G^{(r)j}H^{(r)k}, \tag{2.6c}$$

where the coefficients f, g, and h, owing to the underlying self-similarity, do not depend on r. The above set can be regarded as the RG transformations which enables one to calculate the end-to-end distance critical exponent

$$\nu=\frac{\ln b}{\ln\lambda_\nu}, \tag{2.7}$$

where λ_ν is the largest eigenvalue of the transformations linearized at their nontrivial fixed point [18,19].

The complete description of the adsorption problem requires, in addition to the three bulk restricted partition functions given by Eqs. (2.6), a set of similar nine functions (see Fig. 4) which satisfy the following recursion relations:

$$F_i^{(r+1)}=\sum_{j_1,\ldots,j_{12}} f_i(j_1,\ldots,j_{12})F^{(r)j_1}F_1^{(r)j_2}\cdots F_5^{(r)j_6}G^{(r)j_7}G_1^{(r)j_8}G_2^{(r)j_9}H^{(r)j_{10}}H_1^{(r)j_{11}}H_2^{(r)j_{12}}, \quad i=1,\ldots,5 \tag{2.8a}$$

$$G_i^{(r+1)}=\sum_{j_1,\ldots,j_{12}} g_i(j_1,\ldots,j_{12})F^{(r)j_1}F_1^{(r)j_2}\cdots F_5^{(r)j_6}G^{(r)j_7}G_1^{(r)j_8}G_2^{(r)j_9}H^{(r)j_{10}}H_1^{(r)j_{11}}H_2^{(r)j_{12}}, \quad i=1,2 \tag{2.8b}$$

$$H_i^{(r+1)}=\sum_{j_1,\ldots,j_{12}} h_i(j_1,\ldots,j_{12})F^{(r)j_1}F_1^{(r)j_2}\cdots F_5^{(r)j_6}G^{(r)j_7}G_1^{(r)j_8}G_2^{(r)j_9}H^{(r)j_{10}}H_1^{(r)j_{11}}H_2^{(r)j_{12}}, \quad i=1,2 \tag{2.8c}$$

where the coefficients f_i, g_i, and h_i, are not functions of r, and each of them represents the number of ways in which the part of the SAW path of the corresponding type, within the $(r+1)$th stage fractal structure, can be comprised of the SAW paths within the fractal structures of the next lower order. Because of the independence of r, these coefficients can be calculated by studying all possible SAWs within the fractal generator only.

The above set of relations (2.8), together with Eqs. (2.6), comprise the RG transformations which are needed to determine the crossover critical exponent ϕ. Indeed, it has been shown [11,12,15,16] that one can expect that the RG transformations of the type (2.6) and (2.8) should have three different nontrivial fixed points which correspond to the three different polymer states — the bulk state ($T>T_a$), the crossover state ($T=T_a$), and the adsorbed state ($T<T_a$). At the crossover fixed point (the special fixed point, in the parlance of surface critical phenomena) the two largest eigenvalues λ_ν and λ_ϕ ($\lambda_\nu>\lambda_\phi$) of the linearized RG transformations determine the crossover exponent ϕ [11] through the formula

$$\phi=\frac{\ln\lambda_\phi}{\ln\lambda_\nu}. \tag{2.9}$$

To locate the relevant fixed points of the RG transformations (2.6) and (2.8) we need to specify the initial conditions in terms of the fugacity x and the Boltzmann factors w, t, and u. With this purpose in view, we observe that for any member of the X fractal family the initial conditions can be defined in the case of a unit cross (initiator, $r=0$)

$$F^{(0)}=x^2, \quad F_1^{(0)}=x^2w^2, \quad F_2^{(0)}=x^2wt, \quad F_3^{(0)}=x^2t^2, \quad F_4^{(0)}=x^2wt, \quad F_5^{(0)}=x^2w^2, \tag{2.10a}$$

$$G^{(0)}=x^2, \quad G_1^{(0)}=x^2wt, \quad G_2^{(0)}=x^2w^2, \quad H^{(0)}=0, \quad H_1^{(0)}=0, \quad H_2^{(0)}=0, \tag{2.10b}$$

whereas, in the case of the CB family of fractals (for $b>3$), the initial conditions cannot be formulated for the corresponding initiator (unit square); since relations of type (2.10), upon performing the iteration procedure according to Eqs. (2.6) and (2.8), would imply self-intersections of the SAW path. Therefore, for every CB fractal, the initial conditions have to be established for the fractal generator ($r=1$). We have found the appropriate initial conditions for the $b=5$ and $b=7$ CB fractals. However, the corresponding polynomials in x, w, t, and u contain too many terms. Indeed, there are 12 polynomials with altogether 1967 and 21 689 terms in the case $b=5$ and $b=7$, respectively, which makes it impractical to quote them here.

III. CALCULATION OF THE CROSSOVER EXPONENT

In this section we are going to present both the exact and the MCRG calculation of the crossover exponent ϕ. The exact RG calculation requires knowledge of coefficients f, g, and h of Eq. (2.6) (which were found in [18] for the $3\leq b\leq 9$ fractals), as well as knowledge of coefficients (f_i, g_i, and h_i) of the polynomials (2.8). Using moderate computer facilities, we have been able to calculate the latter coefficients for $b=3$, 5, and 7. We shall first analyze the case $b=3$, and at the beginning we point out that only never-starting and never-ending SAWs are treated in the RG approach applied in this paper. Hence, one can verify that on the $b=3$ fractal (X or CB) infinite SAWs can be performed only by making G type of walks, that is, the partition functions of the F and H type are not relevant. Accordingly, we may put $F^{(r)}=F_i^{(r)}=H^{(r)}=H_i^{(r)}=0$, while for the restricted partition functions of the G type we find

$$G'=G^3, \tag{3.1a}$$

$$G_1'=GG_1G_2, \tag{3.1b}$$

$$G_2'=G_2^3, \tag{3.1c}$$

where we have used the prime symbol as a superscript for the $(r+1)$th order parameters and no indices for the rth order parameters. Henceforth, for the sake of simplicity, we treat only the X fractal case. For the requisite initial conditions, we can use Eqs. (2.10), and thus we find that the above set of the RG transformations has three nontrivial fixed points — ($G=1$, $G_1=0$, $G_2=0$), ($G=0$, $G_1=0$, $G_2=1$),

and ($G=1$, $G_1=t$, $G_2=1$), which, according to numerical investigations of the RG flow [see Fig. 5(a)] correspond, respectively, to the polymer bulk phase, adsorption phase, and to the coexistence of the two phases. Accordingly, in the $b=3$ case, there is no multicritical point which could correspond to the crossover behavior of the polymer system, and, consequently, the critical exponent ϕ is not defined (one can verify that the same situation is valid for the $b=3$ CB fractal).

We have already pointed out that for the $b=5$ and $b=7$ CB and X fractals we have been able to perform exact RG calculations. The corresponding RG transformations (2.6) and (2.8) in the case $b=5$ are given in the Appendix, whereas in the case $b=7$ the pertinent transformations require much more space and we do not give them (the relevant data are, however, available upon requests addressed to the authors).

In the case $b=5$, a numerical analysis of the relations (A1), together with the pertinent initial conditions, reveals existence of the following nontrivial fixed points (with the order of coordinates that corresponds to the order of relevant equations given in the Appendix):

$$(F^*_{(B)},G^*_{(B)},H^*_{(B)},0,0,F^*_{3(B)},0,0,0,0,0,0), \tag{3.2a}$$

$$(F^*_{(B)},G^*_{(B)},H^*_{(B)},F^*_{(B)},F^*_{(B)},F^*_{(B)},F^*_{(B)},F^*_{(B)},G^*_{(B)},G^*_{(B)},H^*_{(B)},H^*_{(B)}), \tag{3.2b}$$

$$(0,0,0,F^*_{1(A)},0,0,0,F^*_{5(A)},0,1,0,0), \tag{3.2c}$$

which we shall term, respectively, the bulk, crossover, and the adsorption fixed point. For the bulk fixed point (3.2a), the first three nonzero coordinates have the values $F^*_{(B)}=0.66371$, $G^*_{(B)}=0.72464$, and $H^*_{(B)}=0.10003$ [18], while the coordinate $F^*_{3(B)}$ is the nontrivial solution 0.477 93 of the equation

$$F^*_{3(B)}=F'_3(F^*_{(B)},G^*_{(B)},H^*_{(B)},0,0,F^*_{3(B)},0,0,0,0,0,0). \tag{3.3}$$

The bulk fixed point can be reached, for the X fractal, starting from $x_c=0.8359$ (or from $x_c=0.5648$ for the CB fractal), and for the relatively small parameter w [see Fig. 5(b)]. The RG transformations (A1), linearized at the bulk fixed point, have only one relevant eigenvalue $\lambda_\nu=6.6077$, which, in conjunction with the formula (2.7), gives $\nu_B=0.852\,35$ [18]. When w reaches the special-point value $w^*(t,u)$ the RG transformations (A1) lead to the crossover fixed point (3.2b), and if one linearizes the RG transformations at this fixed point, one finds two relevant eigenvalues $\lambda_\nu=6.6077$ and $\lambda_\phi=4.091\,10$, which according to Eq. (2.9) gives $\phi=0.746\,10$. Finally, iterations of the RG transformations (A1) that start on a point of the critical line, for $w>w^*(t,u)$ [see Fig. 5(b)], lead to the adsorption point (3.2c) which is characterized by $F^*_{1(A)}=1/F^*_{5(A)}$ in such a way that $F^*_{1(A)}$ is a function of the initial values for w, t, and u. The adsorption fixed point is also characterized by the single relevant eigenvalue $\lambda_A=7$ yielding the end-to-end distance critical exponent $\nu_A=0.827\,09$, which turns out to be equal to $1/d_s$ [see Eq. (2.4) for $b=5$]. The latter result implies that, for the corresponding initial conditions, the adsorbing boundary is completely covered by the polymer.

A numerical investigation of the RG equations in the case $b=7$ confirm the existence of the fixed points of the type (3.2), with the following specific values — $F^*_{(B)}=0.568\,05$, $G^*_{(B)}=0.622\,96$, $H^*_{(B)}=0.058\,49$ [18], and $F^*_{3(B)}=0.416\,33$, while the calculation of the critical exponents gives $\nu_B=0.815\,02$, $\phi=0.644\,87$, and $\nu_A=1/d_s$, where d_s is the fractal dimension of the adsorbing boundary [see Eq. (2.4) for $b=7$].

Exact RG approach to the adsorption problem on the CB and X fractals with $b\geqslant 9$ is a forbidding task using the present day computers, and for this reason we apply the MCRG technique. To learn specific values of the crossover exponent for $b\geqslant 9$, we need to calculate the eigenvalues λ_ϕ [see formula (2.9)], since λ_ν has been already found for a sequence of fractals up to $b=81$ [19] (which appears to be an upper limit for calculations using a computer with the Intel 80860 microprocessor). Calculation of λ_ϕ (for the same sequence of fractals) requires solution of the eigenvalue problem for the RG transformations (2.8) linearized at the crossover fixed point, which in practice necessitates evaluation of 81 partial derivatives of the type $\partial Y'/\partial X$, where X and Y stand for any pair of quantities from the set $\{F_i,G_i,H_i\}$ (calculated at the crossover fixed point). Within an exact RG approach, calculation of these derivatives assumes knowledge of all coefficients f_i, g_i, and h_i, which was a feasible task in the cases $b=5$ and $b=7$. For $b\geqslant 9$, within the MCRG approach, we conceive the quantities F_i, G_i, and H_i, as the grand-canonical partition functions of ensembles of the corresponding SAWs (see Fig. 4). Within this approach the requisite partial derivatives can be written in the form

$$\frac{\partial Y'}{\partial X}=\frac{Y'}{X}\langle N_X\rangle_{Y'}, \tag{3.4}$$

where $\langle N_X\rangle_{Y'}$ is the average number of the SAW elements of the type X, within the fractal generator, calculated in accordance with the grand-canonical ensemble of the type Y. Thus, to find λ_ϕ, we need to solve the eigenvalue problem of the matrix whose elements are the 81 derivatives of the type (3.4) evaluated at the fixed point (3.2b). The coordinates of the crossover fixed points (3.2b) have been found in Ref. [19], so that it remains to evaluate only $\langle N_X\rangle_{Y'}$ at the same

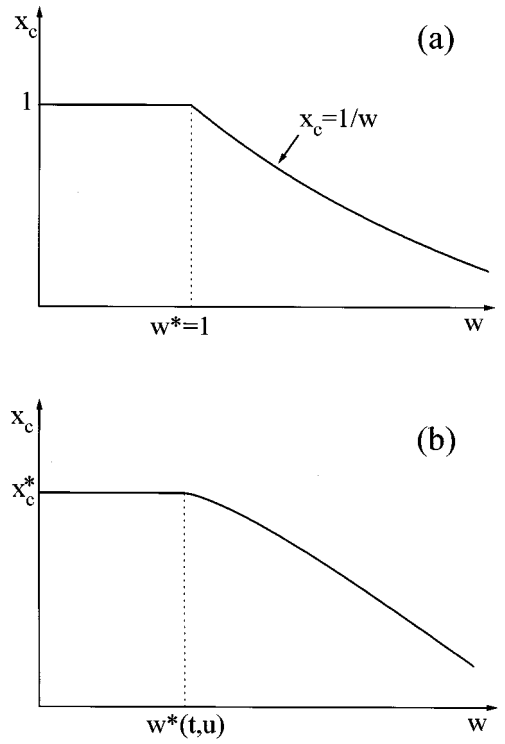

FIG. 5. (a) The critical fugacity x_c curve for the X fractal labeled by $b=3$ as a function of the parameter w for a given t. The RG transformations (3.1) iterated by starting at the horizontal part of the curve lead to the bulk fixed point ($G=1,\ G_1=0,\ G_2=0$), whereas if the iteration starts at the part of the critical fugacity curve $x_c=1/w$ that appears beyond the point ($w^*=1,\ x_c^*=1$), it leads to the adsorption fixed point ($G=0,\ G_1=0,\ G_2=1$). Finally, when the RG iteration starts at the point ($w^*=1,\ x_c^*=1$) it leads to the fixed point ($G=1,\ G_1=t,\ G_2=1$), which corresponds to the first order phase transition. The abrupt increase of the number of adsorbed monomers M, at this fixed point, is related [16] to the discontinuous first order derivative of the singular part of the free energy per monomer $f_{sing}=kT\ln x_c(w,t)$. (b) The critical fugacity curve for the CB and X fractals with $b>3$. Behavior of the RG flow is analogous to the $b=3$ case, except for the point $(w^*(t,u),x_c^*)$ which is now related to the crossover fixed point (3.2b), while the bulk and adsorption fixed points are given by Eqs. (3.2a) and (3.2c), respectively.

fixed point, which, within the MCRG approach, can be directly measured (see, for instance, [15] and references quoted therein). The final results for the crossover critical exponent ϕ, together with the requisite eigenvalues (λ_ν and λ_ϕ), are given in Table I.

TABLE I. The exact ($b=5$ and $b=7$) and the MCRG results ($5\leqslant b\leqslant 81$) for the RG eigenvalue λ_ϕ and the crossover critical exponent ϕ, in the case of the CB (and X) fractals. To make the table complete, we quote also here the eigenvalues λ_ν (obtained in Ref. [19]), which were needed in formula (2.9) to obtain ϕ.

b		λ_ν	λ_ϕ	ϕ
5	exact	6.6077	4.09110	0.746 10
		6.61 ± 0.04	4.094 ± 0.008	0.746 30 ± 0.003 65
7	exact	10.8871	4.629 69	0.644 87
		10.87 ± 0.06	4.627 ± 0.009	0.642 01 ± 0.002 33
9		15.81 ± 0.09	4.925 ± 0.009	0.577 57 ± 0.001 90
11		21.3 ± 0.1	5.13 ± 0.01	0.534 33 ± 0.001 59
13		27.3 ± 0.1	5.24 ± 0.01	0.500 66 ± 0.001 37
15		33.9 ± 0.2	5.33 ± 0.01	0.474 92 ± 0.001 26
19		48.2 ± 0.2	5.43 ± 0.01	0.436 60 ± 0.001 06
23		64.5 ± 0.3	5.50 ± 0.01	0.409 16 ± 0.001 00
25		73.1 ± 0.4	5.47 ± 0.01	0.396 15 ± 0.000 91
27		82.2 ± 0.4	5.52 ± 0.01	0.387 30 ± 0.000 88
35		120.3 ± 0.6	5.50 ± 0.01	0.355 86 ± 0.000 82
43		164.1 ± 0.7	5.52 ± 0.01	0.334 97 ± 0.000 66
51		212 ± 1	5.50 ± 0.01	0.318 19 ± 0.000 74
61		275 ± 1	5.46 ± 0.01	0.302 37 ± 0.000 66
71		346 ± 1	5.48 ± 0.01	0.290 96 ± 0.000 54
81		420 ± 2	5.45 ± 0.01	0.280 85 ± 0.000 54

IV. DISCUSSION AND SUMMARY

In this paper we have presented the exact and MCRG calculations for the crossover critical exponent ϕ which describes the adsorption phenomenon of a linear polymer, in a good solvent, on impenetrable boundaries of fractal containers modeled by the CB (and X) fractal lattices. For the first three members ($b=3,\ 5,\ 7$) of both (CB and X) fractal families we have performed exact RG analysis, which revealed that in the case $b=3$ there is no multicritical behavior described by Eq. (2.5), that is, the crossover exponent ϕ in this case is not defined and the adsorption of monomers is not a continuous critical phenomenon. This implies that in the case $b=3$ the adsorption phenomenon is a first order phase transition, which is accompanied with a jump in the number M of adsorbed monomers [this number is related to the derivative of the critical fugacity; see Fig. 5(a)]. For $b>3$ there appears to be a continuous adsorption of monomers on the corresponding boundaries (whose fractal dimensions $d_s\to 1$, when $b\to\infty$). A similar appearance of an abrupt change to continuous behavior has been observed in the case of adsorption of directed polymers on rough substrates [20]. This appearance has been explained by a decrease in the roughness (which may be related to the self-similarity of the fractal boundaries) of the corresponding adsorbing walls. Finally, it may be appropriate to note that the change in the type of the adsorption phase transition has also been observed in the case of a boundary within a given roughness providing that the monomer-wall interaction in the layer adjacent to the wall may change its intensity [16].

For fractals with $b\geqslant 9$ we have found it formidable to perform exact RG calculations, and thus for a sequence ($5\leqslant b\leqslant 81$) we have applied the MCRG method. The reliability of the MCRG results is manifested by the fact that in the cases $b=5$ and $b=7$ the MCRG results deviate at most 0.15% from the exact results. For the sake of a better assessment of the global behavior of the crossover exponent ϕ as a function of the fractal scaling parameter b, we depict the corresponding values from Table I in Fig. 6. One can see that ϕ, being monotonically decreasing function of b, crosses the two-dimensional Euclidean value $\phi=1/2$ for $b>13$. Besides, one can observe that the phenomenological upper bound $\phi_u=d_s/d_f$, predicted in [11], is always satisfied, whereas the lower bound $\phi_l=1-(d_f-d_s)\nu_B$ [11] is satisfied only in

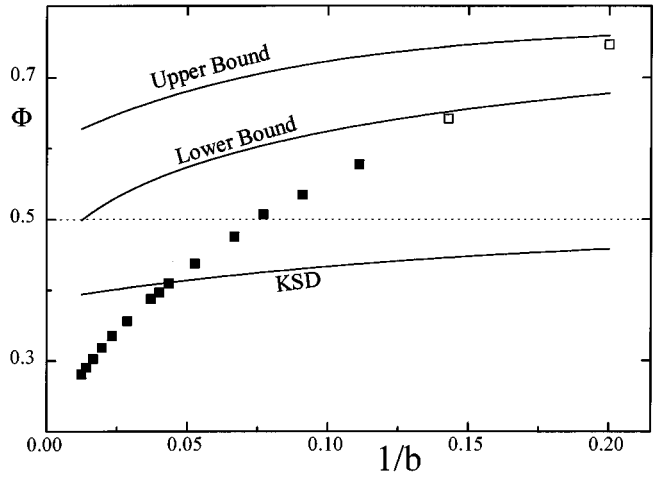

FIG. 6. Data for the crossover critical exponent ϕ for the CB (and X) family of fractals. The exact RG results are represented by open squares, while the MCRG results are depicted by solid squares. The error bars related to the MCRG data are not depicted in the figure since in all cases they lie within the corresponding symbols. The solid curves represent the upper ϕ_u and lower bounds ϕ_l, proposed in [11]. The dashed horizontal line represents the two-dimensional Euclidean value $\phi=1/2$. The lower solid line, labeled by KSD, represents the phenomenological formula $\phi=[1+(1-d_f)\nu_B]/(\nu_B\sqrt{d_f})$ proposed by Kumar, Sing, and Dhar [13].

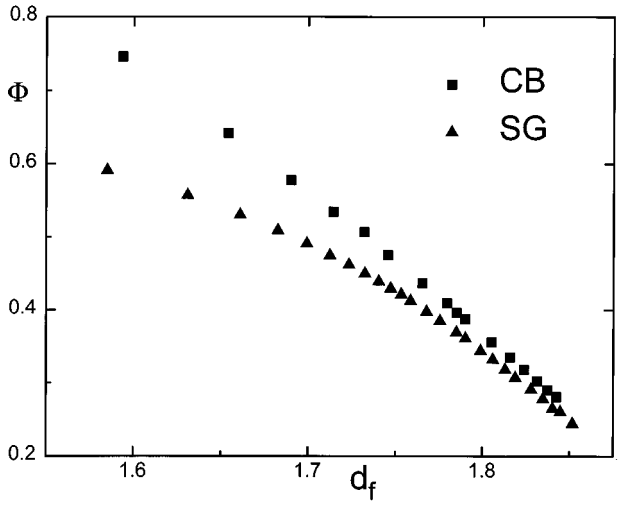

FIG. 7. Data for the polymer adsorption critical exponent ϕ for the CB (and X) family of fractals (solid squares) and for the SG family of fractals (solid triangles) as functions of the corresponding fractal dimensions d_f.

the case $b=5$, which together with previous similar cases (see, for instance, [16] and references quoted therein) calls for a better phenomenological treatment of the adsorption problem on fractal lattices. However, one should not expect that such a treatment can be an easy task, which could be illustrated by the attempt of Kumar, Sing, and Dhar [13] to find a simple phenomenological formula for ϕ in terms d_f and ν_B whose predictions turned to deviate significantly from our exact and MCRG results (see Fig. 6).

It is interesting to see to which extent the obtained results for the crossover exponent ϕ are peculiar to the CB (and X) family of fractals. To this end, we make a comparison with the results obtained previously [11,12,15] for the Sierpinski gasket (SG) family of fractals (see Fig. 7). First, we can observe that, in the region studied, both curves for ϕ monotonically decrease with increasing d_f (that is, with increasing b). This joint property (valid for all three fractal families — CB, X, and SG) can be explained by the fact that the adsorption appears when a balance between the attractive polymer-surface potential and an effective ''entropic'' repulsion sets in. With increasing b the difference in the polymer configurational entropy between the bulk and the adsorbed state increases, while the attractive polymer-surface potential stays relatively constant. This competition obstructs polymer adsorption for larger d_f, which results in decreasing values of ϕ (see Fig. 7). Of course, at this point, one may pose the question whether decreasing of ϕ continues up to very large b, or at a certain $b_{min}>81$ ϕ acquires a minimal value, so that for $b>b_{min}$ it starts to increase. It is hard to answer this question by straightforward calculation of ϕ, but the arguments offered in regard to the similar question for the bulk critical exponent ν_B [19,21] make us conjecture that ϕ may have a minimal value for certain large b, and that for $b\to\infty$ it tends to the Euclidean value 1/2. To vindicate this conjecture it is necessary to pursue further the finite-size scaling arguments initiated by Kumar, Sing, and Dhar [13].

The foregoing comparison of the crossover exponent ϕ for the two different families of fractals (CB or X, versus SG) should be completed by the observation that for a given value of d_f the inequality $\phi_{\mathrm{CB}}>\phi_{\mathrm{SG}}$ holds, which might have been expected on the physical grounds. Indeed, the inequality $\phi_{\mathrm{CB}}>\phi_{\mathrm{SG}}$ should be related to the difference in the fractal dimension d_s of the pertaining impenetrable boundaries. In the SG case $d_s^{\mathrm{SG}}=1$, for each b, whereas d_s^{CB} is given by formula (2.4), so that $d_s^{\mathrm{CB}}>d_s^{\mathrm{SG}}$, which implies that on a same scale of length the CB impenetrable boundary has more adsorbing bonds than the SG boundary. Furthermore, from Fig. 7 it follows that the difference $\phi_{\mathrm{CB}}-\phi_{\mathrm{SG}}$ decreases with increasing b, which is in accord with the fact $d_s^{\mathrm{CB}}\to d_s^{\mathrm{SG}}=1$, when $b\to\infty$. While we are on the subject, we would like to point out the finding that any pair of the CB and X fractals, labeled by the same scaling parameter b, have same values for the crossover exponent despite the fact that the two fractals do not have the same set of monomer-wall interactions (see Fig. 3). On the other hand, the two fractals have the same d_s, for a given b, which demonstrates that the crossover exponent is determined by the configuration of impenetrable boundaries, rather than by the set of the adsorbing interactions.

In conclusion, we may say that, in this study of the polymer adsorption problem on fractal lattices with *fractal* impenetrable boundaries, we have found that the results are qualitatively the same as in the case of fractals with the Euclidean boundaries. On the other hand, the established quantitative differences can be ascribed to the fact that the fractal nature of boundaries do enhance the polymer adsorption process, but with the caution that this enhancement does not depend on specific variations of the sets of monomer-wall interactions.

APPENDIX: THE RG TRANSFORMATIONS FOR THE $b=5$ CB FRACTAL

In this appendix we provide the RG transformations (2.6) and (2.8) in the case of the $b=5$ CB (or X) fractal. For the $b=7$ fractal, the pertinent transformations require much more space and we do not give them here (the relevant data are, however, available upon requests addressed to the authors).

$$F'=F^3G^2+F^7G^2+FG^4+2F^3G^4+3F^5G^4+2F^5G^2H+F^3G^4H+2F^5G^4H+2F^5G^4H^2+3F^5G^2H^3, \tag{A1a}$$

$$G'=6F^4G^3+2F^6G^3+G^5+4F^6G^3H+4F^4G^3H^2+2F^4G^5H^2, \tag{A1b}$$

$$H'=F^6G^4+2F^4G^6+4F^4G^6H+G^8H+6F^6G^4H^2+8F^4G^4H^5, \tag{A1c}$$

$$\begin{aligned}F_1'=&F_1^2F_5G_2^2+2F^3F_1F_5G_2^2H_2+2F^3G^2F_1F_5G_2^2H_2+2F^4HF_5G_2^2H_1H_2+2F^4G^2F_5G_2^2H_1H_2+FG_1^2G_2^2+2F^2GF_2G_1G_2^2\\&+F^3HG_1^2G_2^2+2F^4GF_2G_1G_2^2+F^5F_2^2G_2^2+F^4HF_5G_2^2H_2^2+F^3G^2F_2^2G_2^2,\end{aligned} \tag{A1d}$$

$$\begin{aligned}F_2'=&2F^3G^2F_1F_5G_1G_2+F^4G^2HF_5G_1G_2H_1+F^4G^2F_5G_1G_2H_1+F^4GF_1F_2F_5G_2+2F^3GH^2F_2F_5G_2H_1+G^3F_1F_2F_5G_2\\&+F^3GF_2F_5G_2H_1+F^4G^2F_3G_1G_2+F^2G^2HF_3G_1G_2+F^3G^2G_1G_2+FG^2G_1G_2+F^4GHF_2G_2+F^4G^2HF_5G_1G_2H_2\\&+F^3GH^2F_2F_5G_2H_2+F^3G^3HF_2F_3G_2+F^2GF_2G_2,\end{aligned} \tag{A1e}$$

$$\begin{aligned}F_3'=&F^3G^2+3F^3G^2H^3F_3^2+2F^4G^2H^2F_5G_1^2+2F^3G^3HF_2F_5G_1+2F^4G^2HF_3+F^5G^2F_3^2+2F^2G^4F_3+F^4G^2F_5G_1^2\\&+2F^3G^3F_2F_5G_1+FG^4+G^4HF_2^2F_5,\end{aligned} \tag{A1f}$$

$$\begin{aligned}F_4'=&F^2GF_1F_5^2G_1G_2^2+F^3GHF_5^2G_1G_2^2H_1+FG^2F_1F_2F_5^2G_2^2+F^2G^2F_2F_5^2G_2^2H_1+F^3GF_1F_3F_4F_5G_2+2F^2GH^2F_3F_4F_5G_2H_1\\&+G^3F_1F_4F_5G_2+F^3GF_4F_5G_2H_1+F^3GF_4F_5G_1^2G_2+G^2HF_2F_4F_5G_1G_2+F^2G^2F_3G_1G_2+FG^2G_1G_2\\&+F^3GHF_2F_3G_2+F^3GHF_5^2G_1G_2^2H_2+F^2GH^2F_3F_4F_5G_2H_2+F^2G^2HF_2F_4F_5G_1G_2+F^2GF_2G_2,\end{aligned} \tag{A1g}$$

$$\begin{aligned}F_5'=&FF_2^2G_2^2+2FHF_4^2F_5^2G_2^2H_1H_2+2F^2F_5^3G_2^4H_1H_2+2FGF_2F_4F_5^2G_2^3H_1+2F^2F_2F_4F_5G_2^2H_1+FF_1^2F_4^2F_5^2G_2^2\\&+2GF_1F_4F_5G_1G_2^2+FHF_4^2F_5^2G_2^2H_1^2+F_1^2F_5^3G_2^4+2FF_1F_4F_5^2G_1G_2^3+FG_1^2G_2^2+HF_4^2F_5G_1^2G_2^2,\end{aligned} \tag{A1h}$$

$$\begin{aligned}G_1'=&F^2GF_1F_5G_1G_2+F^4GHF_1F_5G_1G_2+F^3G^3HF_5G_1G_2H_1+FG^2F_1F_2F_5G_2+F^3G^2F_1F_2F_5G_2+F^2G^2HF_2F_5G_2H_1\\&+F^4G^2F_2F_5G_2H_1+F^3GF_3G_1G_2+2F^3GH^2F_3G_1G_2+G^3G_1G_2+F^4GG_1G_2+2F^3G^2F_2G_2+F^5GF_5G_1G_2H_2\\&+F^2G^2HF_2F_5G_2H_2+F^4G^2F_2F_3G_2+F^3G^3HF_5G_1G_2H_2+F^4G^2HF_2F_3G_2,\end{aligned} \tag{A1i}$$

$$\begin{aligned}G_2'=&F_1^2F_5^2G_2^3+2F^3F_1F_5^2G_2^3H_2+2F^2G^2F_5^2G_2^3H_1H_2+2FF_1F_4F_5G_1G_2^2+2F^2GF_1F_2F_4F_5G_2^2+2F^2HF_4F_5G_1G_2^2H_1\\&+2F^3GF_2F_4F_5G_2^2H_1+2F^2HF_4F_5G_1G_2^2H_2+GG_1^2G_2^2+2F^3F_2G_1G_2^2+F^2GF_2^2G_2^2,\end{aligned} \tag{A1j}$$

$$\begin{aligned}H_1'=&F^3G^2F_1^2F_5G_2^2+3F^3G^2H^3F_5G_2^2H_1^2+2F^4G^2HF_1F_5G_2^2H_1+FG^4F_1^2F_5G_2^2+2F^2G^4F_1F_5G_2^2H_1+F^5G^2F_5G_2^2H_1^2\\&+2F^4G^2HF_1F_5G_2^2H_2+4F^3G^2H^3F_5G_2^2H_1H_2+F^4G^2G_1^2G_2^2+G^4HG_1^2G_2^2+2F^3G^3HF_2G_1G_2^2+F^4G^2H^2F_2^2G_2^2\\&+F^3G^2H^3F_5G_2^2H_2^2,\end{aligned} \tag{A1k}$$

$$\begin{aligned}H_2'=&2F^4G^2HF_1F_5G_2^2H_2+6F^3G^2H^3F_5G_2^2H_1H_2+2F^2G^4F_1F_5G_2^2H_2+2F^5G^2F_5G_2^2H_1H_2+2F^3G^3HF_2G_1G_2^2+G^4HG_1^2G_2^2\\&+2F^3G^3F_2G_1G_2^2+2F^4G^2H^2F_2^2G_2^2+2F^3G^2H^3F_5G_2^2H_2^2+F^4G^2F_2^2G_2^2.\end{aligned} \tag{A1l}$$

[1] For a review, see D. Napper, *Polymeric Stabilization of Colloidal Dispersions* (Academic, New York, 1983); G.P. de Gennes, Adv. Colloid Interface Sci. **27**, 189 (1987); M. Kawaguchi and A. Takahashi, *ibid.* **37**, 219 (1992).
[2] A résumé has been given by K. Binder and K. Kremer, in *Scaling Phenomena in Disordered Systems*, edited by R. Pynn and A. Skjeltrop (Plenum, New York, 1985), p. 525; for a more recent review, see K. De' Bell and T. Lookman, Rev. Mod. Phys. **65**, 87 (1993).
[3] T. W. Burkhardt, E. Eisenriegler, and I. Guim, Nucl. Phys. B **316**, 559 (1989).
[4] H. Meirovitch and I. Chang, Phys. Rev. E **48**, 1960 (1993).
[5] I. Guim and T. W. Burkhardt, Phys. Rev. E **49**, 1495 (1994).
[6] P. Grassberger and R. Hegger, J. Phys. A **27**, 4069 (1994).
[7] P. Grassberger and R. Hegger, Phys. Rev. E **51**, 2674 (1995).
[8] H. Meirovitch and I. Chang, Phys. Rev. E **51**, 2677 (1995).
[9] P. Fendley and H. Saleur, J. Phys. A **27**, L789 (1994).
[10] M. T. Batchelor and C. M. Yung, Phys. Rev. Lett. **74**, 2026 (1995).
[11] E. Bouchaud and J. Vannimenus, J. Phys. (Paris) **50**, 2931 (1989).
[12] V. Bubanja, M. Knežević, and J. Vannimenus, J. Stat. Phys. **71**, 1 (1993).
[13] S. Kumar, Y. Sing, and D. Dhar, J. Phys. A **26**, 4835 (1993).
[14] S. Kumar and Y. Sing, Phys. Rev. E **48**, 734 (1993).
[15] I. Živić, S. Milošević, and H. E. Stanley, Phys. Rev. E **49**, 636 (1994).
[16] V. Miljković, S. Milošević, and I. Živić, Phys. Rev. E **52**, 6314 (1995).
[17] E. Eisenriegler, K. Kremer, and K. Binder, J. Chem. Phys. **77**, 6296 (1982).
[18] S. Elezović-Hadžić and S. Milošević, J. Phys. A **25**, 4095 (1992).
[19] S. Milošević and I. Živić J. Phys. A **26**, 7263 (1993).
[20] G. Giugliarelli and A. L. Stella, Phys. Rev. **53**, 5035 (1996).
[21] S. Milošević and I. Živić, in *Diffusion Processes: Experiment, Theory, Simulations*, edited by A. Pekalski (Springer-Verlag, Berlin, 1994), p. 137.